

Ultrafast photogeneration of charged polarons in conjugated polymers

Paulo B. Miranda, Daniel Moses, and Alan J. Heeger*

Institute for Polymers and Organic Solids, University of California at Santa Barbara, Santa Barbara, California 93106

(Received 17 January 2001; revised manuscript received 2 April 2001; published 2 August 2001)

Ultrafast photoinduced absorption by infrared-active vibrational modes (IRAV) is used to detect charged photoexcitations (polarons) in conjugated luminescent polymers. The experiments, carried out in zero applied electric field, show that polarons are generated instantaneously (within ~ 100 fs) with appreciable quantum efficiencies, $\phi_{\text{ch}} \sim 10\%$. The ultrafast photoinduced IRAV absorption, the weak pump-wavelength dependence of ϕ_{ch} and linear dependence of charge density on pump intensity indicate that both charged polarons and neutral excitons are independently generated even at the earliest times. Several mechanisms for charge generation proposed in the literature are eliminated by these results.

DOI: 10.1103/PhysRevB.64.081201

PACS number(s): 77.84.Jd, 71.20.Rv, 78.47.+p, 78.30.Jw

Semiconducting (conjugated) polymers have been known for over twenty years. Research on these materials has intensified in the last decade as a result of the increasing number of applications, including light-emitting diodes, lasers, and solar cells.¹ Despite many advances, the nature of the elementary excitations in semiconducting polymers remains controversial.² Issues of great importance to the understanding and improvement of polymer devices, such as the exciton binding energy and charge carrier generation mechanism, remain unresolved. Here we use a unique all-optical technique^{3,4} based on photoinduced infrared-active vibrational (IRAV) modes to study the photogeneration and recombination dynamics of charged polarons in poly(paraphenylene-vinylene) (PPV) and its derivatives.

There are two dominant theoretical views of the charge generation mechanism in conjugated polymers.^{2,5} The first is based on the model of Su, Schrieffer and Heeger (SSH),⁶ which treats the polymer chain as a tight-binding one-dimensional semiconductor in the one-electron approximation and explicitly includes the electron-phonon interaction. The SSH approach assumes that the electron-electron (el-el) interactions are relatively weak because of screening, leading to small exciton binding energies (≈ 0.1 eV).⁷ The coincidence of the onset of absorption and photoconductivity has been used as support for this approach, where charges are directly photogenerated. In the second theoretical approach, the el-el interactions are assumed to be dominant so that bound excitons with relatively large binding energy (≥ 0.4 eV) are the elementary photoexcitations. Charged polarons are then indirectly generated by mechanisms such as exciton dissociation by electric fields^{5,8,9} or defects,^{10,11} exciton bimolecular decay,¹² hot-exciton dissociation,¹³ sequential excitation to higher lying states,¹⁰ and carrier photoinjection from electrodes.⁵ Studies of excitations generated at high-photon energies relative to the onset of π - π^* absorption are particularly important for resolving these issues. For excitations generated at high-photon energies, the excitonic states would be more delocalized, facilitating exciton dissociation and leading to a significant increase in the efficiency for charge generation, ϕ_{ch} .^{14,15} Therefore, a direct measurement of the dependence of ϕ_{ch} on the excitation wavelength is particularly important for clarification of the charge generation mechanism.

The traditional technique used to investigate the charge generation process in conjugated polymers is photoconductivity (PC). However, since PC is dependent on carrier generation efficiency, mobility and lifetime, the interpretation is not straightforward.^{4,5} Xerographic discharge experiments⁸ might allow more direct interpretation, but they probe charge generation in the millisecond time scale, and therefore do not address the early-time photoexcitations. Here we use ultrafast photoinduced IRAV absorption, an all-optical technique with subpicosecond time resolution carried out in zero applied electric field, to investigate the charge generation mechanism in PPV and its soluble derivatives.^{3,4} The IRAV absorption results from Raman-active vibrational modes that become infrared-active when the local symmetry is broken by self-localization of charges (polaron formation). The IRAV modes have a 1:1 correspondence with the strongest modes observed on resonant Raman scattering and have an unusually high infrared absorption cross section ($\sigma_{\text{IRAV}} \sim 10^{-16}$ cm², comparable to electronic transitions).^{1,6,16} They are a well-known probe of photo- or doping-induced charged excitations (solitons, polarons, and bipolarons) in conjugated polymers and have been described in detail elsewhere.^{6,17,18} Thus, photoinduced IRAV absorption can address the question of whether charged polarons are photogenerated at ultrafast time scales in conjugated polymers. There is, however, an important distinction between the charges detected by IRAV absorption and by PC. While the latter charges must be mobile, IRAV absorption is also sensitive to charges in localized states that do not contribute to PC.¹⁹

The samples were freestanding films with thickness from 1 to 40 μm . We have studied stretch-aligned PPV (draw-ratio $1/I_0=4$) and disordered films of PPV derivatives, such as MEH-PPV (poly[2-methoxy-5-(2'-ethyl)hexyloxy-1,4-phenylene vinylene]) and BuEH-PPV (poly[2-butyl-5-(2'-ethyl)hexyl-1,4-phenylene vinylene]), prepared by multiple spin casting from 1% w/v toluene solutions onto sapphire substrates, and subsequently removed from the substrate. For comparison and quantitative determination of the quantum efficiency, we used the MEH-PPV/C₆₀ blend (50% w/w of the C₆₀ derivative 1-(3-methoxycarbonyl)propyl-1-phenyl[6,6], C₆₁).

The optical setup consisted of an amplified Ti:Sapphire system (wavelength 795 nm, 1 mJ/pulse, ~ 100 fs pulse du-

ration, 1 kHz repetition rate) pumping two optical parametric amplifiers (OPA's). The first OPA was used to pump the samples and generated pulses tunable between 600 nm to 250 nm by nonlinear mixing of pump, signal, and idler beams. Additional pump wavelengths were obtained by third- and fourth-harmonic generation of the fundamental wavelength. The second OPA was equipped with a difference-frequency generation stage and generated the probe beam, tunable from 3 to 10 μm (1000 to 3300 cm^{-1}). The pump and probe pulses overlapped on the sample and the delay between them was controlled with a variable delay line. Polarizations were linear and parallel, with the IR polarized along the stretch direction of the PPV sample. The differential changes in transmission [$\Delta T/T = (T_{\text{on}} - T_{\text{off}})/T_{\text{off}}$] of the probe induced by the pump beam were measured as a function of the pump-probe delay (t). The smallest detectable signal was $\Delta T/T = 10^{-3}$, and the typical excitation density was of the order of 10^{19} cm^{-3} . The experiments were carried out at room temperature in a vacuum chamber with pressure less than 10^{-5} torr. Each measurement of $\Delta T/T(t)$ was fit to a convolution of multiple exponential decays and a Gaussian representing the temporal resolution of the experiment.²⁰ From the fit, we extracted the initial differential transmission $\Delta T/T(0)$, which is related to the quantum efficiency for charge pair generation (ϕ_{ch}) by $\Delta T/T(0) = 2 \phi_{\text{ch}} \sigma F$, where F is the photon flux absorbed by the sample (photons/ cm^2) and σ is the cross section for IRAV absorption.

There is direct experimental evidence that neutral bound-state excitations, such as intrachain^{5,21} or interchain^{22,23} excitons, do not contribute to the measured photoinduced IRAV absorption. First, the addition of C_{60} to MEH-PPV is known to promote ultrafast electron transfer from the polymer to C_{60} , yielding a positive polaron in the polymer and an electron in C_{60} .²⁴ For high enough C_{60} concentrations, this process has quantum efficiency close to 100% and leads to nearly complete luminescence quenching and increased PC (with charge collection efficiencies higher than 60%).²⁵ Previous reports demonstrated that the ultrafast IRAV signal is enhanced by a factor ~ 3 when adding 50% by weight of C_{60} to MEH-PPV.⁴ If excitons were contributing to the mid-IR absorption, however, the signal would have been reduced by exciton quenching. From the ratio of IRAV signals in pristine MEH-PPV and the MEH-PPV/ C_{60} blend, the quantum efficiency for charge pair generation in pristine MEH-PPV when pumped at 400 nm was estimated as $\sim 10\%$ (assuming the electron transfer efficiency in the blend to be 100%). Moreover, the different dynamics of the IRAV photoinduced absorption and the stimulated emission in MEH-PPV under identical excitation conditions¹⁹ indicates that excitons cannot be the major contribution to the IRAV signal.

Figure 1 shows the spectra of the IRAV modes obtained with steady-state excitation for the MEH-PPV/ C_{60} blend, and with the ultrafast setup for both MEH-PPV and the MEH-PPV/ C_{60} blend. The steady-state and ultrafast spectra are in reasonable agreement, with all the spectral features present in both. They are also in good agreement with the data obtained at ~ 100 ps time resolution.³ The ultrafast photoinduced IRAV modes demonstrate that polarons are

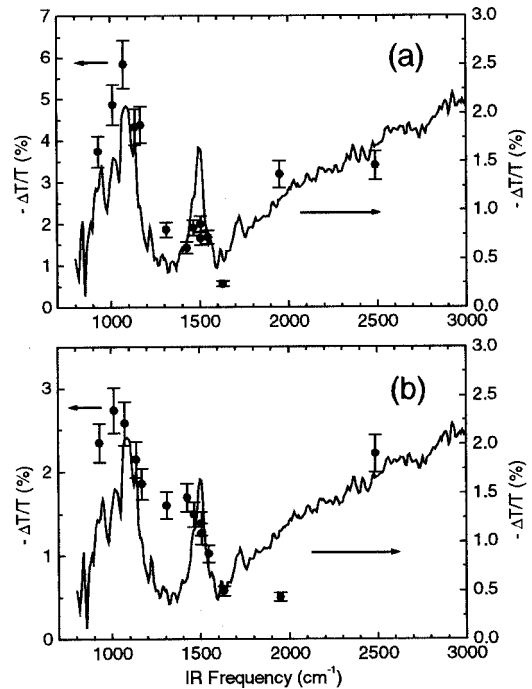


FIG. 1. Photoinduced IRAV spectrum for (a) MEH-PPV/ C_{60} blend and (b) pristine MEH-PPV. Solid circles are the ultrafast measurements at “ $t=0$ ” and $T=300$ K. For comparison, the solid line in both (a) and (b) is the steady-state IRAV spectrum for the MEH-PPV/ C_{60} blend ($T=90$ K). The pump wavelength was 494 nm and 514 nm for the ultrafast and steady-state measurements, respectively.

produced in less than 100 fs, consistent with the early predictions of Su and Schrieffer.²⁶

Figure 2 shows the excitation spectrum for ultrafast charge generation for stretch-oriented PPV and for MEH-PPV (not oriented) from the onset of absorption up to 6.2 eV (filled circles). The most striking feature is the weak dependence of ϕ_{ch} over such a wide range of photon energies: PPV shows a modest increase above 3.5 eV, which is not observed in MEH-PPV. Data obtained from BuEH-PPV (not shown) were very similar to those from MEH-PPV. Figure 2 shows that the product $\sigma \cdot \phi_{\text{ch}}$ is about twice larger in *chain-aligned* PPV than in MEH-PPV when pumped on the main absorption peak. Although different interchain interactions might play a role,^{19,28} this is more likely a result of the alignment of the PPV chains in contrast to the random orientation in MEH-PPV. This should enhance σ by a factor of two since the IRAV absorption is polarized parallel to the polymer chain. Thus, with $\phi_{\text{ch}} \sim 10\%$ for MEH-PPV,⁴ Fig. 2(a) shows that $\phi_{\text{ch}} \sim 35\%$ at pump energies above 4 eV, implying that under such conditions charged polarons are a very significant fraction of the photoexcitations in the polymer. Indeed, Ruseckas *et al.*²⁸ have independently shown that charged polarons are generated within ~ 100 fs with $\phi_{\text{ch}} \sim 20\%$ in a polythiophene derivative. They suggested that these charges are interchain pairs, with oppositely-charged polarons residing on neighboring chains. Although we cannot conclusively address the intra-*versus* interchain nature of the charge pairs, we emphasize they cannot be in a bound state.

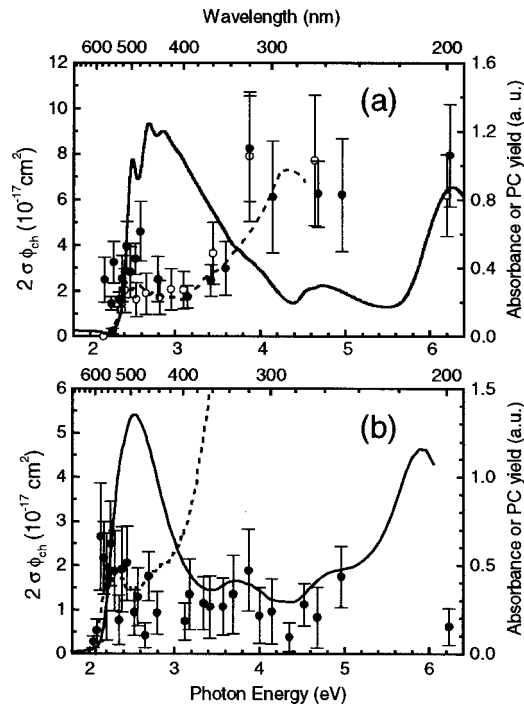


FIG. 2. Charge photogeneration excitation spectrum for (a) PPV and (b) pristine MEH-PPV. Solid circles are the ultrafast measurements (IR probe at 1100 cm^{-1}) and solid lines are the sample absorption spectrum [the spectrum in (a) was taken from Ref. 27]. Dashed lines are steady-state PC action spectra [curve in (b) was taken from Ref. 15]. The empty circles in (a) are transient PC measurements.

It is interesting to compare these results with previous PC measurements in MEH-PPV. The dashed line in Fig. 2(b) is the steady-state PC action spectrum taken from Ref. 15, obtained with a sandwich cell configuration. It shows a much more pronounced increase in the ultraviolet than our direct measurements of ϕ_{ch} . An even larger increase can be found in Ref. 14. Similar results were obtained for PPV-ether and PPV-amine derivatives.⁵ These PC measurements are, in fact, the only strong experimental support of the notion of strongly-bound excitons. Because this strong increase is not observed in the excitation spectrum of ϕ_{ch} , we have performed transient and steady-state PC measurements using the more reliable surface electrode geometry²⁹ on the stretch-aligned PPV film, with both the electric field and light polarization parallel to the polymer chains. The results are also shown in Fig. 2(a). In contrast to earlier reports for related systems, there is good agreement between the ultrafast IRAV and the transient and steady-state PC measurements. The only difference appears at the onset of absorption, where the IRAV measurements indicate that charges are generated, but no photocurrent is detected. We conclude that these charges are in disorder-induced localized states that cannot contribute to conductivity, but do generate IRAV absorption. The enhanced charge generation near the onset of π - π^* absorption in MEH-PPV [Fig. 2(b)] is consistent with increased disorder in the spin-cast film.¹⁹ The weak wavelength dependence of ϕ_{ch} for MEH-PPV is also consistent with xerographic discharge data obtained at high electric fields with millisecond time resolution.⁸

The weak wavelength dependence of ϕ_{ch} and the ultrafast nature of charge generation ($<100\text{ fs}$) imply that charged polaron pairs are directly photogenerated at all photon energies above the onset of π - π^* absorption. Furthermore, we have observed a linear dependence on pump intensity for both ultrafast IRAV and stimulated emission signals (probing charge and exciton densities, respectively). These results eliminate several indirect charge generation mechanisms proposed in the literature. Since these measurements were performed with no applied electric field on a pristine free-standing film, field-induced exciton dissociation and photo-injection from electrodes are not possible. It has also been suggested that bimolecular exciton annihilation would be responsible for charge generation at high optical excitation densities.¹² However, the linear intensity dependence of the charge density is in disagreement with this notion. Although a strong bimolecular decay of the stimulated emission (SE) is observed at high intensities (initial decay $\sim 2\text{ ps}$), the rise-time of the photoinduced IRAV signal is always resolution-limited. Therefore, bimolecular decay of excitons is not a significant source of charges. Sequential two-photon excitation of highly energetic excitons has been proposed as a mechanism for ultrafast charge generation at high excitation intensities.¹⁰ However, in order to have a linear intensity dependence of the charge density, this mechanism requires a saturation of the low-energy exciton density, which is not observed in our experiments (data not shown). Moreover, there is no sign of the resonance expected from the sequential two-photon mechanism as the pump energy is tuned through the absorption band. Furthermore, this mechanism

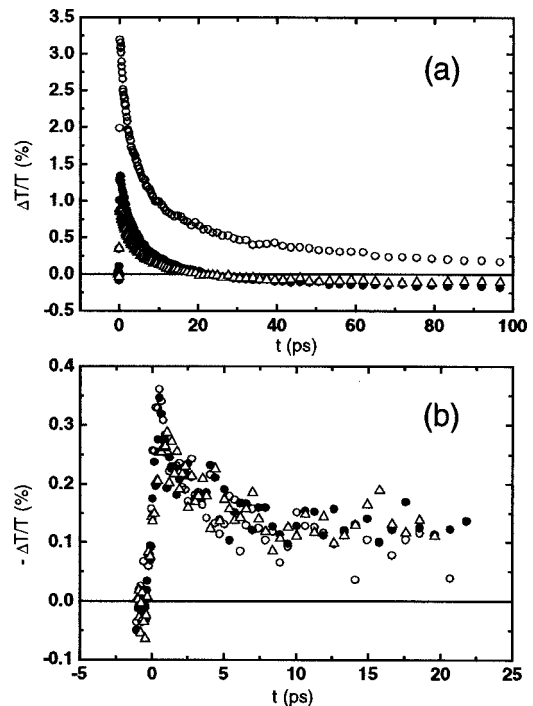


FIG. 3. Sequence of three measurements of (a) SE at 633 nm and (b) IRAV photoinduced absorption at 1100 cm^{-1} , for MEH-PPV pumped at 482 nm . Empty circles are for a pristine sample in vacuum. Solid circles and empty triangles are two consecutive measurements with the sample in air.

assumes that charge generation is considerably more efficient upon excitation at high-photon energies, also in disagreement with the results in Fig. 2. Hot-exciton dissociation¹³ is still another mechanism proposed to explain charge generation in the presence of electric fields, where phonons emitted upon relaxation of the initial excited state into a bound exciton form a thermal bath that induces exciton dissociation before the vibrational cooling time. It could still lead to ultrafast charge generation in zero electric field, although the charges would eventually recombine into a bound exciton again. However, in order to explain the weak wavelength dependence of ϕ_{ch} , its magnitude and the ultrafast charge generation with reasonable parameters, the exciton binding energy has to be small (<0.1 eV).

Exciton dissociation at defect sites was proposed to explain the ultrafast generation of charged polarons.¹⁰ The results in Fig. 3 address this issue. A pristine MEH-PPV sample, prepared and handled in inert atmosphere, was studied in vacuum and then purposely photooxidized. The pristine sample showed SE [Fig. 3(a)] that persisted at long delay times (> 50 ps). Upon photo-oxidation, a photoinduced absorption competed with and overcame the SE at long delays, as observed before by others.³⁰ Yet, the IRAV absorption was not changed beyond our experimental accuracy under the same conditions. These data demonstrate that exciton dissociation by photo-oxidized defects is not required for significant charge generation and that at least at modest defect densities, ϕ_{ch} is not affected by photo-oxidation. In more highly photo-oxidized samples, there is a significant increase in the steady-state PC (Ref. 31) from a combination of in-

creased ϕ_{ch} , carrier mobility and/or lifetime, which complicates the interpretation of PC measurements. Calculations have suggested that conformational defects could be responsible for ultrafast charge generation.¹¹ However, the similar results obtained from spin-cast films of MEH-PPV and from chain-oriented PPV are not consistent with this hypothesis.

Finally, the dynamics of the photoinduced IRAV absorption is generally nonexponential and quite short-lived [a typical example is shown in Fig. 3(b)] but it depends significantly on the initial excitation density, with larger densities leading to shorter decays. This is indeed what should be expected for charged polaron pair recombination, which happens within tens of picoseconds in the conditions of our experiments.

In conclusion, these experiments have shown that polarons are generated in conjugated polymers within ~ 100 fs with appreciable quantum efficiencies ($\sim 10\%$) that are only weakly dependent on the excitation wavelength. The data are not consistent with indirect charge generation by excitons of large binding energy. It is clear that both excitons and polarons are independently generated even at times less than 100 fs. The mechanism responsible for this intrinsic ultrafast branching of the photoexcitations into neutral excitons and charged polarons remains to be elucidated.

We thank C. Silva, T. K. Däubler, L. J. Rothberg, Z. V. Vardeny, and B. J. Schwartz for useful discussions, A. Dogariu for help with the initial experiments, and M. Stevenson for assistance with sample preparation. This research was supported by the National Science Foundation (NSF-DMR 9812852).

*Corresponding author. Email: ajh@physics.ucsb.edu. Present address: Physics Department and Materials Department, UCSB.

¹M. D. McGehee *et al.*, in *Advances in Synthetic Metals*, edited by P. Bernier (Elsevier, Lausanne, 1999), p. 98.

²N. S. Sariciftci, *The Nature of Photoexcitations in Conjugated Polymers* (World Scientific, Singapore, 1997).

³U. Mizrahi *et al.*, *Synth. Met.* **102**, 1182 (1998).

⁴D. Moses *et al.*, *Phys. Rev. B* **61**, 9373 (2000).

⁵S. Barth and H. Bässler, *Phys. Rev. Lett.* **79**, 4445 (1997).

⁶A. J. Heeger *et al.*, *Rev. Mod. Phys.* **60**, 781 (1988).

⁷N. Kirova *et al.*, *Synth. Met.* **100**, 29 (1999).

⁸T. K. Däubler *et al.*, *Adv. Mater.* **11**, 1274 (1999).

⁹W. Graupner *et al.*, *Phys. Rev. Lett.* **81**, 3259 (1998).

¹⁰C. Silva *et al.*, *Synth. Met.* **116**, 9 (2001).

¹¹H.-F. Meng and T.-M. Hong, *Phys. Rev. B* **61**, 9913 (2000).

¹²G. J. Denton *et al.*, *Synth. Met.* **102**, 1008 (1999).

¹³V. I. Arkhipov *et al.*, *Phys. Rev. Lett.* **82**, 1321 (1999).

¹⁴A. Köhler *et al.*, *Nature (London)* **392**, 903 (1998).

¹⁵M. Chandross *et al.*, *Phys. Rev. B* **50**, 14 702 (1994).

¹⁶C. R. Fincher Jr. *et al.*, *Phys. Rev. B* **19**, 4140 (1979).

¹⁷B. Horowitz, *Solid State Commun.* **41**, 729 (1982).

¹⁸Z. G. Soos *et al.*, *J. Chem. Phys.* **100**, 7144 (1994).

¹⁹Details will be published elsewhere.

²⁰Our previous experiments had a time resolution of ~ 100 fs. (Ref. 4). Here we focus on different issues, and our present time resolution varies from 300 to 500 fs due to uncompensated dispersion in the vacuum chamber BaF₂ window.

²¹N. T. Harrison *et al.*, *Phys. Rev. Lett.* **77**, 1881 (1996).

²²M. Yan *et al.*, *Phys. Rev. Lett.* **72**, 1104 (1994).

²³H. A. Mizes *et al.*, *Phys. Rev. B* **50**, 11 243 (1994).

²⁴N. S. Sariciftci *et al.*, *Science* **258**, 1474 (1992).

²⁵G. Yu *et al.*, *Science* **270**, 1789 (1995).

²⁶W. P. Su and J. R. Schrieffer, *Proc. Natl. Acad. Sci. U.S.A.* **77**, 5626 (1980).

²⁷D. Comoretto *et al.*, *Phys. Rev. B* **62**, 10 173 (2000).

²⁸A. Ruseckas *et al.*, *Chem. Phys. Lett.* **322**, 136 (2000).

²⁹D. Moses, *Phys. Rev. B* **53**, 4462 (1996).

³⁰T.-Q. Nguyen *et al.*, *J. Phys. Chem. B* **104**, 237 (2000).

³¹H. Antoniadis *et al.*, *Phys. Rev. B* **50**, 14 911 (1994).